



## Preparation of bamboo activated carbon by microwave radiation with water vapour activation and investigation of its adsorption properties

Xiuying Fang<sup>†</sup>, Min Yang<sup>†</sup>, Jiaxiong Li, Mu Xiang, Kaini Yang, Hongbin Wang\*, Guizhen Li\*

Key Laboratory of Resource Clean Conversion in Ethnic Regions, School of Chemistry and Environment, Yunnan Minzu University, Kunming, 650500, China, email: 1197084904@qq.com (X. Fang), 826677468@qq.com (M. Yang), 243990096@qq.com (J. Li), 2927655249@qq.com (M. Xiang), 1549840437@qq.com (K. Yang), wanghb2152@126.com (H. Wang), 325865775@qq.com (G. Li)

Received 2 May 2018; Accepted 12 August 2018

### ABSTRACT

The bamboo activated carbon (BAC) was prepared from bamboo charcoal, a commercial product, using microwave radiation with water vapour activation. The surface chemistry and physical characteristics of BAC were investigated by scanning electron microscope (SEM), Brunauer-Emmett-Teller surface area (BET) analyzer, X-Ray Diffraction (XRD), Thermogravimetric differential scanning calorimetry (TG-DSC) curve and fourier transform infrared spectroscopy (FT-IR). The BAC was used for the removal of p-nitrophenol in water. The operational variables including adsorbent dosage, pH, concentration and temperature of solution on the adsorption processes were studied. The BAC regeneration experiments were also carried out. The results showed that the iodine adsorption value was 1099 mg/g and the carbon yield was 34.3% under the optimum conditions. The BAC had a specific surface area of 1168.72 m<sup>2</sup>/g, total pore volume of 2.203 mL/g and micropore volume of 0.444 mL/g. The removal rate could reach 84% under the BAC dosage of 30 mg and p-nitrophenol solution pH of 5.33. The results of kinetic studies and isothermal adsorption model showed that pseudo-second-order kinetics and Langmuir isothermal adsorption model was well fitted the adsorption equilibrium process. After four times of regeneration, the removal rate could still reach 72%.

*Keywords:* Bamboo activated carbon; P-nitrophenol; Water vapour activation; Microwave radiation; Adsorption

### 1. Introduction

Bamboo resource is an important part of forest resources. China is the country with the most abundant bamboo resources in the world. The species of bamboo, the area of bamboo forest and the accumulation of bamboo resources are the first in the world, which is known as the “bamboo kingdom”. According to Zhida Zhang [1], the total area of bamboo forests around the world is about 14 million ha with more than 850 species. There are more than 500 species of bamboo species known in China, with an area of 3.79 million hectares of bamboo. They accounted for 60% and 27% of the world bamboo species and bamboo forest area, respectively.

Water pollution has been a global environmental issue. Phenol wastewater is a concern among industrial wastewater. Most of the phenol compounds are toxic. With the increases of amount and types of phenol-containing waste waters, the phenol wastewater treatment has become a research hot topic in the field of water pollution control [2]. At present, the treatment methods of phenol wastewater mainly include oxidation [3], extraction [4], biological degradation [5,6] and adsorption method [7,8], etc. Adsorption treatment of wastewater has the characteristics of well treatment effect, recyclable and reusable. The activated carbon with good chemical stability, special pore structure and surface functional groups [9] has been widely used in adsorption treatment of wastewater pollutants [10].

\*Corresponding author.

<sup>†</sup>These two authors contributed equally to this work.

Presented at the 10th International Conference on Challenges in Environmental Science & Engineering (CESE-2017), 11–15 November 2017, Kunming, China

In this study, bamboo charcoal was used as a raw material for the preparation of activated carbon adsorbent by microwave irradiation and water vapor activation. The adsorption performance (activation temperature, time and particle size) was investigated. The adsorption properties of p-nitrophenol were studied by using this adsorbent, and aiming to remove p-nitrophenol contamination.

## 2. Materials and methods

### 2.1. Preparation of BAC

Bamboo charcoal used in the experiments was carbonized material, which was purchased from Wind Boat Chemical Reagent Technology Co., Tianjin, Ltd. It was placed in microwave tube furnace and heated to a predetermined temperature in a nitrogen atmosphere with the heating rate of 5–10°C/min. then water vapor with a flow rate of 6.4 g/min was introduced for a certain period of time, which was termed water vapor activation. After activation, nitrogen gas was introduced to prevent oxidize. The product was subsequently dried in an oven at 120°C for 24 h.

### 2.2. Characterization of BAC

The porous structure of BAC was determined by nitrogen (N<sub>2</sub>) adsorption-desorption isotherm at 77 K using automatic volumetric adsorption analyzer (Micromeritics, Model ASAP 2020, USA). The specific surface area was calculated by the Brunauer-Emmett-Teller (BET) equation. The surface morphology was observed by scanning electron microscopy (SEM) analyzer (Model NOVA NANOSEM 450, FEI of USB). The surface chemical functional groups were obtained by Fourier transform infrared (FT-IR) spectrometer (Model IS10, NICOLET). The number and structure of micro crystalline were measured by X-ray diffractometer (XRD) analyzer (Model D8AA25X, BROCK of GER). The temperature-dependent weight loss rate was measured with Netzsch STAA49F31 thermal analyzer.

### 2.3. Adsorbates

The iodine and methylene blue were selected as the model adsorbates, which were obtained from Fangzheng Reagent Factory, Beichen District, Tianjin. The properties of iodine and methylene blue are shown in Table 1, respectively.

p-nitrophenol was purchased from Aladdin's Reagent. It was selected the process objects in this work because

of its wide water pollution. The properties and molecular structure of p-nitrophenol are shown in Table 1 and Fig. 1, respectively.

A standard solution of 2 g/L was prepared by dissolving an appropriate quantity of p-nitrophenol in distilled water. Working solutions of desired concentrations were prepared by successive dilution.

### 2.4. Analysis methods

The iodine and methylene blue adsorption values were carried out according to GB/T 12496.1-12496.22-1999 [11,12], which are for the characterisation of wooden activated carbon.

The adsorption of p-nitrophenol on BAC was determined by measuring p-nitrophenol concentration in filtrate using UV-Vis spectrophotometer (Model 8453, Agilent of USA) at a wavelength of 318 nm.

### 2.5. Batch adsorption experiments

Batch adsorption experiments were carried out by employing different parameters such as adsorbent dosage (5–70 mg), pH (3–13), time (0–180 min), temperature (25–45°C) and the initial concentration of p-nitrophenol (80–320 mg/L). The mixture was kept in a thermostated mechanical shaker to reach equilibrium with an agitation speed of 240 rpm, filtered and the concentration of p-nitrophenol in the filtrate was analyzed using UV-vis spectrophotometer at 318 nm. The amount of adsorbate adsorbed at equilibrium,  $q_e$  (mg/g) was calculated using Eq. (1).

$$q_e = \frac{C_0 - C_e}{M} \times V \quad (1)$$

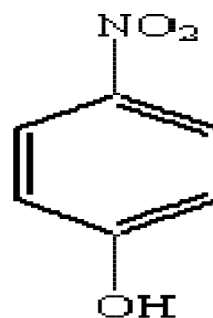


Fig. 1. Molecular structure of p-nitrophenol.

Table 1  
Physical and chemical properties of adsorbates

Adsorbates	Iodine	Methylene blue	p-nitrophenol
CAS number	7553-56-2	7220-79-3	100-02-7
Molecular mass (g/mol)	253.81	373.90	139.11
Purity (%)	99.8	98.5	99
Molecular formula	I <sub>2</sub>	C <sub>16</sub> H <sub>18</sub> ClN <sub>3</sub> S·3H <sub>2</sub> O	C <sub>6</sub> H <sub>5</sub> NO <sub>3</sub>
$\lambda_{\max}$ (nm)	–	–	318

where  $C_0$  (mg/L) is the initial concentration of p-nitrophenol, whereas  $C_e$  (mg/L) represent equilibrium concentration of p-nitrophenol,  $V$  (ml) is the volume of the solution of p-nitrophenol and  $M$  (mg) is the amount of adsorbent used.

The batch experiments for the adsorption kinetics were similar to that of the equilibrium studies. The experiments were conducted at different time intervals and the concentrations of p-nitrophenol were measured using the same technique. The amount of p-nitrophenol adsorbed at time  $t$ , at  $q_t$  (mg/g) and the removal efficiency of p-nitrophenol,  $R$  (%) were calculated by Eqs. (2) and (3) respectively.

$$q_t = \frac{C_0 - C_t}{M} \times V \quad (2)$$

$$R(\%) = \frac{C_0 - C_t}{C_0} \times 100 \quad (3)$$

where  $C_0$  (mg/L) is the initial concentration of p-nitrophenol and  $C_t$  (mg/L) is the concentration of p-nitrophenol at time  $t$ .  $V$  (ml) is the volume of the solution of p-nitrophenol and  $M$  (mg) is the amount of adsorbent used, and  $R$  is the p-nitrophenol removal efficiency in (%).

### 3. Results and discussion

#### 3.1. Preparation of BAC

##### 3.1.1. Effects of activation temperature

Table 2 shows the iodine and methylene blue adsorption values of BAC prepared with different activation temperature (800–950°C). As can be seen from Table 2, the iodine adsorption value increased from 696 mg/g to 938 mg/g and methylene blue value increased from 4 mL/0.1 g to 13.5 mL/0.1 g with the increase of activation

temperature from 800°C to 950°C. This increase in adsorption values may be due to that water vapor first reacted with the tar residue in the carbonized material to remove the partially disordered carbon, then reacted with the carbon skeleton to generate new pore structure [13]. The pore structure was not fully developed at low temperature, but the increase of temperature promoted the endothermic reaction between carbon and water vapor, which was favorable for the formation of new pores [14]. Nevertheless, the corresponding carbon yield decreased significantly from 57.6% to 37% with the increasing temperature from 800°C to 950°C. This decrease in yield may be due to the increase in losing of volatile material at high temperatures [15]. Thus, 950°C has been taken as best activation temperature for preparation.

##### 3.1.2. Effects of activation time

Table 3 showed the iodine and methylene blue value of BAC prepared with different activation time (10–50 min). It can be seen from Table 3 that the iodine adsorption value first increased from 815 mg/g to 1107 mg/g, thereafter it decreased from 1107 mg/g to 989 mg/g, and the methylene blue adsorption value increased from 0.70 mL/0.1 g to 14.2 mL/0.1 g with the prolonging of activation time from 10 min to 50 min. the iodine adsorption value reached the maximum with the activation time of 20 min. This change may be explained by the fact that in the initial stage of activation, which facilitated the rudimentary opening of pores, during pyrolysis and development of new pores [16]. After a long period of activation, pore-widening played a major role, whereas pore-deepening and the formation of new pore play secondary roles, thus more meso pores and macro pores are evolved. The corresponding carbon yield decreased from 65% to 16% with the prolong of activation time from 10 min to 50 min, which might be due to the oxidation reaction of bamboo charcoal and the higher the

Table 2

Effects of activation temperature (particle size of 2–3 mm and activation time of 20 min)

Activation temperature (°C)	Iodine adsorption value $C_0$ (mg/g)	Iodine adsorption value $C$ (mg/g)	Methylene blue adsorption value (mL/0.1 g)	Carbon yield (%)
800	148	696	4	57.6
850	148	757	5.2	52
900	148	868	9.8	46
950	148	938	13.5	37

Table 3

Effects of activation time (particle size of 2–3 mm)

Activation time (min)	Iodine adsorption value $C_0$ (mg/g)	Iodine adsorption value $C$ (mg/g)	Methylene blue adsorption value (mL/0.1 g)	Carbon yield (%)
10	148	815	7	65
20	148	1107	13.1	48
30	148	1035	13.5	32
40	148	1024	14	29
50	148	989	14.2	16

degree of carbonized material by erosion [17]. Therefore, 20 min can be considered as optimum activation time for preparation of BAC in this work.

### 3.1.3. Effects of the particle size

Table 4 shows the iodine and methylene blue adsorption value of BAC prepared with different particle size (2–15 mm). As can be seen from Table 4, the iodine adsorption value (from 820 mg/g to 1099 mg/g) and methylene blue adsorption value (from 8.1 mL/0.1 g to 14.3 mL/0.1 g) increased with the decrease of particle size, and the corresponding carbon yield showed a decreasing trend (from 49% to 34%). In a certain range of particle size, the decrease of particle size can make the contact of raw materials and water vapor more fully, so that the activator can be effectively utilized in the activation process [18]. Thus, the particle size of 2–3 mm was selected as the best experimental particle size.

### 3.2. Comparison of performance of BAC obtained with different methods

As can be seen from Table 5, the two heating methods of the preparation process comparison shows that microwave radiation had the advantages of short activation time. The activation temperature stage, the microwave radiation could reached up to the required temperature in only a few minutes. However, high-temperature activation need nearly 90 min to achieve the required activation temperature, the activation time was longer, it was 2.5 times of the microwave radiation. In addition, the iodine and methylene blue adsorption value was better than the high temperature activation, which exceeded the national standard, and high

temperature activation could only activate about 30 g of bamboo charcoal at a time, but microwave method could activate about 100 g of bamboo charcoal at a time. Therefore, microwave radiation and water vapor activation were selected for subsequent research.

### 3.3. Characterization of bamboo activated carbon

#### 3.3.1. SEM analysis

Fig. 2 shows the SEM images of bamboo charcoal (a) and BAC (b) with magnification of 180000 times. It can be clearly observed from Fig. 2, the surface of bamboo charcoal was relatively smooth, and nevertheless, the surface of BAC was uneven. It indicates that BAC using water vapor activation had abundant and dense pore structures. The increase porosity after activation also reflected in the increased surface area of BAC [19].

#### 3.3.2. BET analysis

The surface areas and pore structure parameters analyzed by BET are shown in Table 6. The BAC had a specific surface area of 1168.72 m<sup>2</sup>/g, micro pore surface area of 1030.37 m<sup>2</sup>/g, external surface area of 138.35 m<sup>2</sup>/g, average pore size of 2.786 nm, total pore volume of 2.203 cm<sup>3</sup>/g and micro pore volume of 0.444 cm<sup>3</sup>/g. The results indicate that water vapor promoted the formation of pore structures, and the above results are consistent with the SEM results [20].

#### 3.3.3. FT-IR analysis

Fig. 3 depicts the FTIR spectra of the bamboo charcoal (a) and the BAC (b). Fig. 3 shows that the intense band was

Table 4  
Effects of the particle size

Particle sizes (mm)	Iodine adsorption value C <sub>0</sub> (mg/g)	Iodine adsorption value C (mg/g)	Methylene blue adsorption value (mL/0.1 g)	Carbon yield (%)
15–20	148	820	8.1	49
10–15	148	893	9.9	42
5–10	148	961	12.5	38
3–5	148	990	13	37
2–3	148	1099	14.3	34

Table 5  
Comparison of performance of BAC obtained with different methods

Conditions and indicators	Microwave radiation	High-temperature activation	First class standard
Temperature (°C)	950	850	
Time (min)	20	50	
Steam flow rate (g/min)	6.4	2.65	
Particle size (mm)	2–3	2–3	
Iodine adsorption value (mg/g)	1099	1038	1000
Methylene blue adsorption value (mL/0.1 g)	14.3	12	9
Carbon yield (%)	34	39	

at about  $3400\text{ cm}^{-1}$ , which was ascribed to the O-H stretching vibration. There may be the hydroxyl groups in carboxyl group, phenol and alcohol. The band at  $1600\text{ cm}^{-1}$  was corresponded to the C=O stretching vibration of the carbonyl ester, ketone, carboxylic acid or the C=C stretching vibration of the unsaturated hydrocarbon compound; the band at  $1100\text{ cm}^{-1}$  was corresponded to the C-O stretching vibration of the alcohol or ester; the band  $1440\text{ cm}^{-1}$  and  $600\text{--}1000\text{ cm}^{-1}$  was corresponded to the existence of aromatic ring [21]. At  $3400\text{ cm}^{-1}$ , the decrease of the O-H of BAC was obvious, which may result in the pyrolysis of the group during the activation process. At  $1600\text{ cm}^{-1}$ , the number of carboxyl groups increased significantly. The result indicated that the BAC had abundant functional groups.

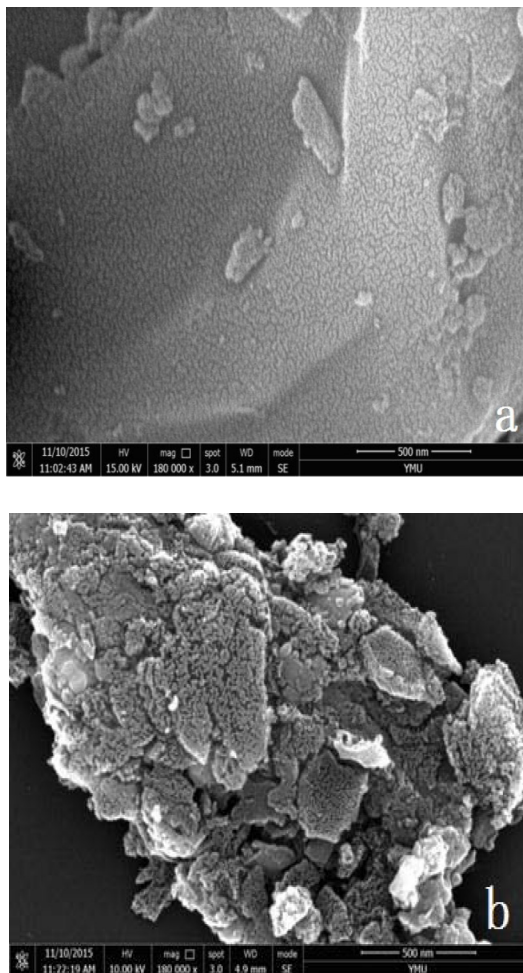


Fig. 2. SEM images of bamboo charcoal (a) and BAC (b) with magnification of 180000 times.

Table 6  
Date of the pore size distribution of BAC

Surface area ( $\text{m}^2/\text{g}$ )	Micropore area ( $\text{m}^2/\text{g}$ )	External surface area ( $\text{m}^2/\text{g}$ )	Average pore radius(nm)	Total pore volume ( $\text{cm}^3/\text{g}$ )	Mircopore volume ( $\text{cm}^3/\text{g}$ )
1168.72	1030.37	138.35	2.786	2.203	0.444

### 3.3.4. XRD analysis

The patterns of bamboo charcoal (a) and BAC (b) are shown in Fig. 4. The measured XRD pattern of bamboo charcoal (a) had similarity to the XRD pattern of BAC (b). The diffraction peaks located around  $25^\circ$  and  $44^\circ$ , which was consistent with data reported in Refs [22]. The  $2\theta$  at  $25^\circ$  correspond to the (002) diffraction plane of graphite structure, and  $2\theta$  at  $44^\circ$  correspond to the (100) diffraction plane of graphite structure, which was consistent with date reported in Refs [23]. From Fig. 4 it is obvious that the peaks around  $2\theta = 25^\circ$  and  $2\theta = 44^\circ$  slightly increased for the BAC. This change may be explained by the fact that the number

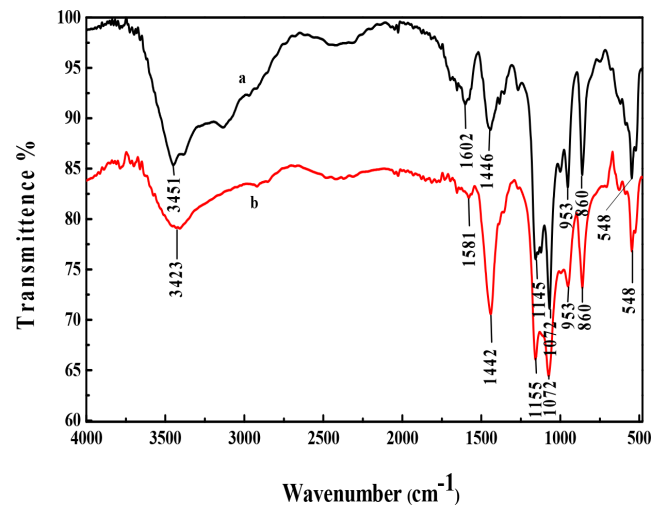


Fig. 3. FTIR spectra of bamboo charcoal (a) and the BAC (b).

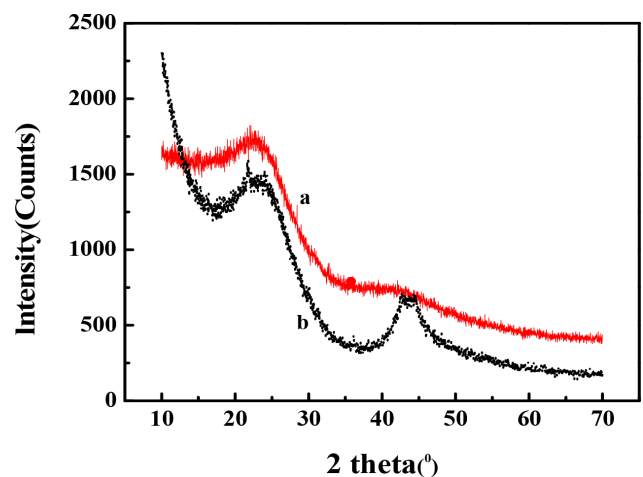


Fig. 4. XRD pattern of bamboo charcoal (a) and BAC (b).

of graphite crystalline in carbon materials increased with the increase of carbonization or activation temperature and the prolongation of heating time. Nevertheless, the carbonization temperature was between 300–600°C and the activation temperature was between 700–1000°C, thus the diffraction peaks of BAC was stronger than that of bamboo charcoal.

### 3.3.5. TG-DSC analysis

The TG-DSC curves of bamboo charcoal and BAC are shown in Fig. 5. The significant weight loss of bamboo charcoal and BAC was about 3% and 8% at 20–100°C, respectively. At this stage the weight loss was mainly caused by the evaporation of water. The second stage of weight loss of bamboo charcoal at 350–920°C, the weight loss was about 95%. The second stage of weight loss of BAC at 300–720°C, the weight loss was about 86%. The weight loss in this period was mainly caused by the cellulose and lignin pyrolysis of raw materials, in addition, it also caused by the dehydrogenation condensation of aromatic compounds. According to the DSC curve of bamboo charcoal and BAC, the DSC curves of the two graphs had endothermic peak

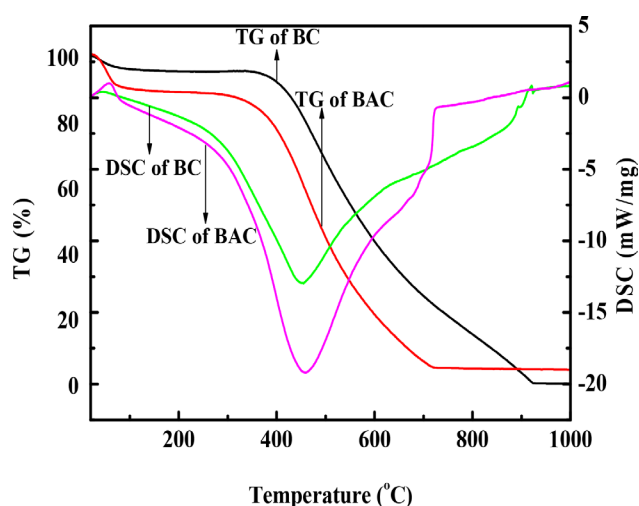


Fig. 5. Characteristic curves of bamboo charcoal: TG (a) and DSC (b).

at about 460°C, which coincides with the change of the TG curve [24].

### 3.4. Comparison of performance parameters of activated carbons with other works

The performance parameters of activated carbons from different studies are listed in Table 7. The comparison indicates that the performance parameter (Surface area, Total pore volume, Iodine adsorption values) obtained in this work was comparable with the previous researches. The high surface area and iodine adsorption value observed in this work demonstrates the energy saving potential and effectiveness of microwave heating generation mechanism.

### 3.5. Batch adsorption experiments

#### 3.5.1. Effect of adsorbent dosage on adsorption of p-nitrophenol

As shown in Fig. 6, removal efficiency of p-nitrophenol was also significantly affected by adsorbent dosage. The removal efficiencies of p-nitrophenol increase from 20% to

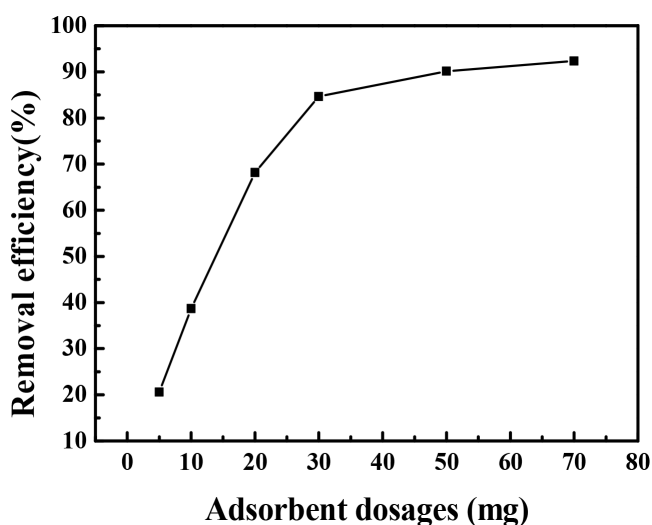


Fig. 6. Characteristic curves of BAC: TG (a) and DSC (b).

Table 7

Comparison of performance parameters of activated carbons with other works

Feedstock	Activator	Surface area, BET (m <sup>2</sup> /g)	Total pore volume (cm <sup>3</sup> /g)	Iodine adsorption values (mg/g)	Refs
Camellia nutshell	ZnCl <sub>2</sub>	2023.15	2.34	1120	(Zhou, 2014)
Arundo donax L.	H <sub>4</sub> P <sub>2</sub> O <sub>7</sub>	1443.4	1.333	–	(Sun, 2014)
Camellia nutshell	Steam	935	–	968	(Zhou and Zhang, 2003)
Bamboo	Steam	1068	0.55	–	(Zhang, 2015)
Rubber wood sawdust	Steam	1092	–	765	(Prakash Kumar et al., 2006)
Phenolic Resin	Steam	727.62	–	1050.28	(Zhao et al., 2009)
Bamboo charcoal	Steam	1168.72	2.203	1099	This work

84% with ranges of adsorbent dosage from 5 mg to 30 mg. This might be due to increases in surface area of the adsorbent with the increase in adsorbent dosage [25]. Further, it was noticed that increasing adsorbent dosage does not show any increase in removal efficiency. This may be due to fact that all active sites may be occupied by adsorbent and the overlapping of active sites at higher dose [26].

3.5.2. Effect of pH on adsorption of p-nitrophenol

Adsorption is also affected by the pH change of the solution [27]. Fig. 7 depicts that percentage removal of p-nitrophenol first reduced and then increased with the increase of pH, the percentage removal was relatively good (pH < 5.5 or pH > 9.5), but relatively poor (pH = 5.5–9.5). This might be due to the amount of H<sup>+</sup> in the solution is more under low pH (<5.5), and the nitro group is the electron-withdrawing group, so that the electro negativity of the oxygen atom in the phenolic hydroxyl group is strengthened, the positive charge of the hydrogen atom is strengthened, which increases the hydrogen bonding sites [28]. The pH

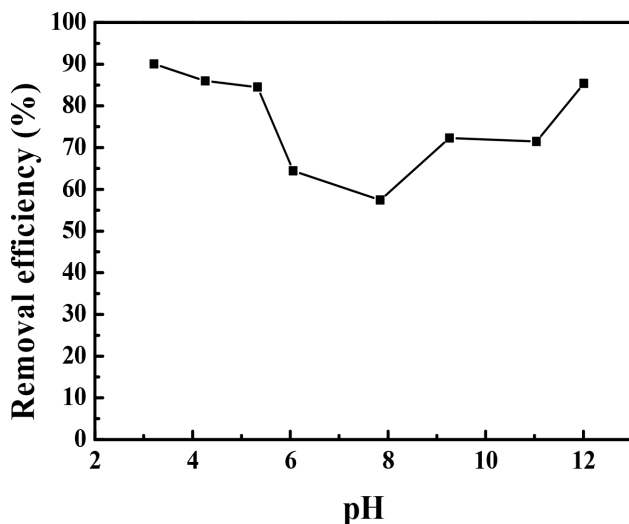


Fig. 7. Effect of adsorbent dosage on the removal efficiency of p-nitrophenol using BAC ( $V = 50$  ml,  $C_0 = 160$  mg/L, pH = 5.33,  $T = 298$  K).

of p-nitrophenol solution was 5.33. The percentage removal was 84% at this pH. Therefore, it does not adjust the pH of p-nitrophenol solution in the follow-up experiments.

3.5.3. Adsorption kinetics

In order to better explain the adsorption mechanism and behavior of p-nitrophenol during the adsorption process that Lagergren pseudo-first-order and McKay pseudo-second-order kinetic models were used to analyze the experimental data and the calculated adsorption capacity was compared with the actual amount that the coincidence degree of the fitting equation was investigated.

(i) The linear expression of Lagergren’s pseudo-first order kinetic model [29] is given by:

$$\text{Log}(q_e - q_t) = \text{Log}q_e - \frac{k t}{2.303} \tag{4}$$

In the above equation  $q_e$  (mg/g) is the amount of p-nitrophenol adsorbed at equilibrium,  $q_t$  (mg/g) is the amount of p-nitrophenol adsorbed at time  $t$  (min),  $k_1$  ( $\text{min}^{-1}$ ) is the Lagergren rate constant of pseudo-first-order adsorption and  $t$  (min) is the contact time.

(ii) The linear form if the Ho’s pseudo-second-order kinetic model [30,31] is given by:

$$\frac{t}{q_t} = \frac{1}{k_2 q_e^2} + \frac{t}{q_e} \tag{5}$$

where  $k_2$  (g/mg/min) is the equilibrium rate constant of pseudo-second-order adsorption.  $q_t$  (mg/g) is the p-nitrophenol adsorbed at a given time period ( $t$ ),  $q_e$  (mg/g) is the p-nitrophenol adsorbed at equilibrium.

The kinetic parameters are listed in Table 8. It can be seen from Table 8 that the correlation coefficients  $R^2_{adj}$  of the pseudo-second-order kinetic model are greater, which indicates that the pseudo-second-order kinetic model fitted to describe the adsorption process better. In addition, the calculated values of  $q_e$  agreed well with the measured values of  $q_e$ , the relative error was less than 1.93%. In this process, there existed the behavior of surface adsorption, liquid film diffusion and particle diffusion. It also can be seen from Table 8 that the adsorption capacity had a decreased tendency with the increase of temperature, which indicates that low temperature was beneficial to the removal of p-nitrophenol.

Table 8 Comparison adsorption rate constants of first order and second order and calculated and experimental  $q_e$

Variable		Pseudo-first order kinetic model				Pseudo-second order kinetic model		
		$q_e$ (exp) (mg/g)	$q_e$ (cal) (mg/g)	$k_1/\text{min}^{-1}$	$R^2_{adj}$	$q_e$ (cal) (mg/g)	$k_2$ (g/mg/min)	$R^2_{adj}$
T/K	298	218.9	5.082	0.0002	0.3907	218.9	0.02086	0.9999
	308	210.9	6.642	0.0058	0.8497	215.0	0.02703	1
	318	208.4	2.535	0.0003	0.0624	211.6	0.44664	0.9999
$C_0/\text{mg/L}$	80	121.7	1.720	0.0051	0.6664	121.9	0.07474	1
	160	218.9	5.920	0.0014	0.3122	218.9	0.01896	0.9999
	240	270.7	10.22	0.0032	0.5264	278.3	0.06454	0.9999
	320	298.1	4.500	-0.0041	0.7283	311.3	0.00368	0.9995

### 3.5.4. Adsorption isotherm

Adsorption isotherm is beneficial for describing the interaction of adsorbates with adsorbents. Therefore, it is critical for the optimal utilization of adsorbents. In this study, Langmuir and Freundlich isotherm models were applied to simulate the isotherm data.

#### 3.5.4.1. Langmuir isotherm model:

Langmuir isotherm model [32] is based on the following assumptions: (i) adsorption cannot proceed beyond mono layer coverage, (ii) all surface sites are equivalent and can accommodate only one adsorbate molecule, and (iii) the ability of a molecule to adsorb at a given site is independent of the occupation of neighboring sites. The nonlinear expression of the Langmuir isotherm model is given by:

$$q_e = \frac{KLq_m}{1 + KLC_e} \quad (6)$$

and one of its linear equations is given in Eq. (7):

$$\frac{1}{q_e} = \frac{1}{K_L q_m} \times \frac{1}{C_e} + \frac{1}{q_m} \quad (7)$$

where  $C_e$  (mg/L) is the concentration of p-nitrophenol at equilibrium,  $q_e$  (mg/g) is the adsorption capacity at equilibrium,  $q_m$  (mg/g) gives the maximum adsorption capacity at complete coverage,  $K_L$  (L/mg) is the Langmuir adsorption equilibrium constant that related to the free energy of adsorption.

#### 3.5.4.2. Freundlich isotherm model:

Freundlich isotherm model [33] predicts the heterogeneous surface adsorption sites of adsorbents. The nonlinear expression of the the Freundlich isotherm model is given by Eq. (8):

$$q_e = K_f C_e^{1/n} \quad (8)$$

The logarithmic linear form of the equation is given in Eq. (9):

$$\ln q_e = \frac{1}{n} \ln C_e + \ln K_f \quad (9)$$

where  $K_f$  is Freundlich constant related to the adsorption capacity,  $n$  are Freundlich parameters related to the adsorption intensity. It can be calculated from the linear plots of  $\ln q_e$  vs.  $\ln C_e$ .

The adsorption isotherms of p-nitrophenol from solution on the BAC (at 25°C, 35°C and 45°C, respectively) are depicted in Fig. 8. The similar shapes of the isotherms suggest that the adsorption process occurred via the similar pathways. As shown in Fig. 8, the initial isotherms rise rapidly during the initial stage of adsorption when  $C_e$  and  $q_e$  values are both lower, there are many readily accessible sites available on the surface of BAC [34]. However, the adsorption isotherms rate of decrease gradually at high concentrations, it is due to more time is required to reach to equilibrium [35].

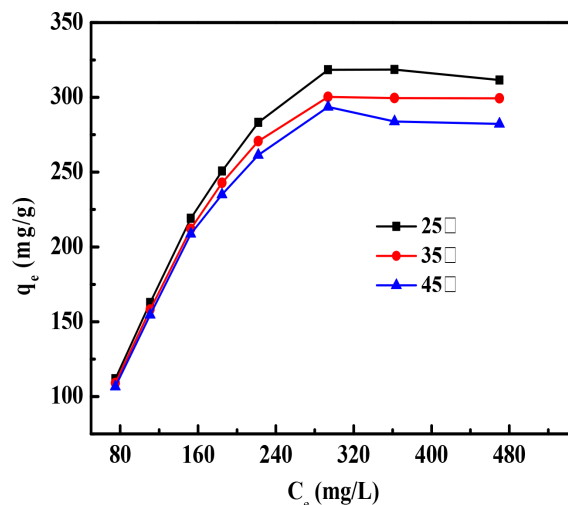


Fig. 8. The effect of pH on the removal efficiency of p-nitrophenol using BAC ( $V = 50$  ml,  $C_0 = 160$  mg/L,  $T = 298$  K, adsorbent dosage = 30 mg).

The corresponding parameters and correlation coefficients are listed in Table 9 and the result of Langmuir is shown in Fig. 9a, and the result of Freundlich is shown in Fig. 9b. Applicability of the isotherm models to describe the adsorption process was judged by the correlation coefficient ( $R^2$ ) values.

It can be seen from Table 9 that the adsorption behavior of BAC on p-nitrophenol could best fitted to the Langmuir isotherm model, because Langmuir isotherm has the higher correlation coefficient, which indicates that the adsorption behavior of BAC on p-nitrophenol is monolayer adsorption.

### 3.5.5. Thermodynamic studies

The physical or chemical nature of adsorption of p-nitrophenol on the BAC was predicted by estimating the thermodynamic parameters. Thermodynamic parameters such as free energy ( $\Delta G$ ), enthalpy ( $\Delta H$ ) and entropy ( $\Delta S$ ) were estimated by taking different temperature and were calculated by the following equations.

$$\Delta G = -RT \ln K \quad (10)$$

$$\Delta G = \Delta H - T\Delta S \quad (11)$$

$$\ln K = \frac{\Delta S}{R} - \frac{\Delta H}{RT} \quad (12)$$

where  $R$  (8.314 J/mol/K) is the universal gas constant and  $T$  (K) is the reaction temperature.  $K$  (L/mg) is the distribution coefficient for the adsorption.

All thermodynamic parameters are shown in Table 10. The negative values of  $\Delta G$  at all temperature indicate spontaneous nature for the adsorption process. The negative  $\Delta H$  reveals the exothermic reaction of BAC adsorption. The degree of randomness increased as value of  $\Delta S$  is negative. All these results were observed by Ahmed [36] using micro porous activated carbon.

Table 9  
Langmuir and Freundlich isotherm model parameters

T/K	Langmuir isotherm model				Freundlich isotherm model			
	Equation	$q_{max}$ (mg/g)	$K_L$ (L/mg)	$R^2$	Equation	$1/n$	$K_f$	$R^2$
298	$q_e = \frac{20.85C_e}{1 + 0.0566C_e}$	369.0	0.05653	0.9858	$q_e = 83.09C_e^{0.2698}$	0.2698	83.09	0.7775
308	$q_e = \frac{16.90C_e}{1 + 0.04496C_e}$	349.4	0.04496	0.9833	$q_e = 75.34C_e^{0.2761}$	0.2761	75.34	0.7775
318	$q_e = \frac{16.66C_e}{1 + 0.05165C_e}$	322.6	0.05165	0.9048	$q_e = 72.02C_e^{0.2735}$	0.2735	72.02	0.7467

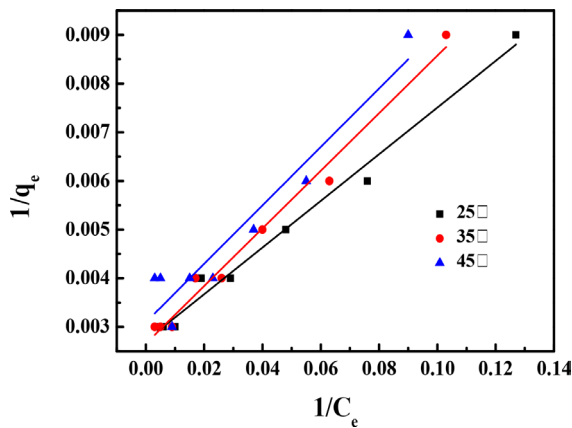


Fig. 9a. Langmuir isotherm plots for the adsorption of p-nitrophenol on BAC.

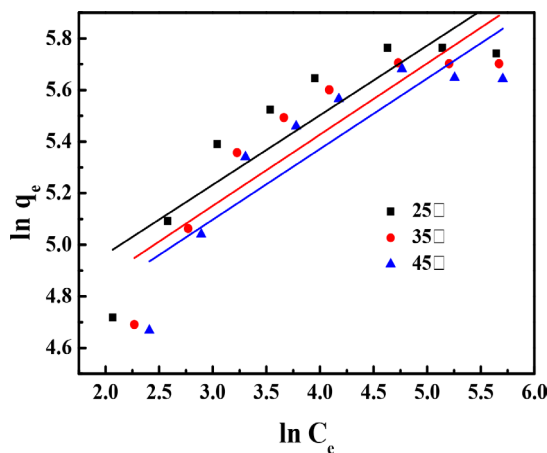


Fig. 9b. Freundlich isotherm plots for the adsorption of p-nitrophenol on BAC.

3.6. Regeneration of BAC

The effect of microwave regeneration on the percentage removal of p-nitrophenol was shown in Fig. 10. It can be seen from Fig. 10 that the initial percentage removal of BAC was 84%. After four adsorption-regeneration cycles, the per-

Table 10  
Thermodynamic parameters for the adsorption of p-nitrophenol on BAC at different temperatures

Temperature (°C)	$\Delta G$ (KJ/mol)	$\Delta H$ (J/mol)	$\Delta S$ (J/mol/K)
25	-17.32	-3711.95	-36.83
35	-17.75		
45	-18.26		

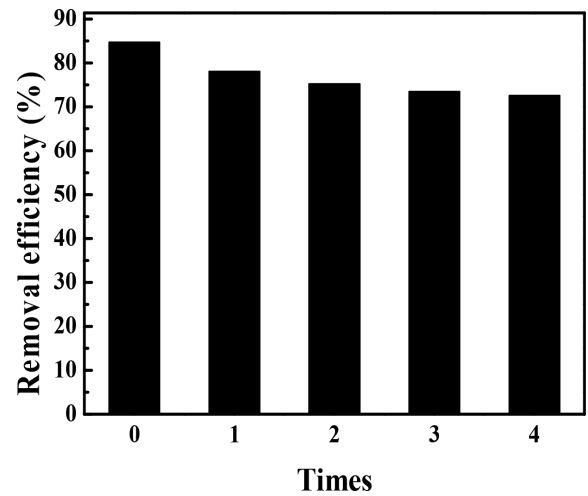


Fig. 10. Effect of regeneration times.

centage removal of p-nitrophenol could still reach 72%. The result indicates the performance of BAC by microwave-assisted regeneration is well, integration of microwave irradiation promoted the preservation of porosity and adsorption performance in a short heating period [37]. Meanwhile, the study demonstrates the effectiveness of microwave heating for regeneration of BAC.

4. Conclusions

The results of the study demonstrate the potential of bamboo charcoal as an efficient raw material for the preparation of BAC via microwave radiation and water vapor activation. The surface morphology, adsorption perfor-

mance, carbon yield, oxygen-containing functional groups and porosity of BAC were significantly affected by the activation conditions. Optimum conditions for the preparation of BAC include the mass of 100 g, water vapor flow rate of 6.4 g/min, activation temperature of 950°C, activation time of 20 min and particle size of 2–3 mm. The BAC had a good adsorption performance, with the iodine adsorption and methylene blue adsorption value of 1099 mg/g and 14.3 mL/0.1 g, respectively; it also had a developed porous structure with the BET surface area of 1168.72 m<sup>2</sup>/g, micro pore area of 1030.37 m<sup>2</sup>/g and total pore volume of 2.203 cm<sup>3</sup>/g. The results showed that BAC had a good potential for the removal of p-nitrophenol from wastewater. In this work, the maximum percentage removal was 84% at pH = 5.33, due to the increased the concentration of H<sup>+</sup> on BAC surface. The temperature exhibits a negative effect on the percentage removal of p-Nitro phenol. It was found that adsorption equilibrium was better described by Langmuir isotherm model, with a monolayer adsorption capacity of 320 mg/g. Further, the adsorption kinetic shows that the process was best fitted with pseudo-second order model. Meanwhile, the study demonstrates the effectiveness of microwave heating for the regeneration of BAC.

#### Acknowledgments

This work was financially supported by YMU-DEAKIN International Associated Laboratory on Functional Materials, Key Laboratory of Resource Clean Conversion in Ethnic Region, Education Department of Yunnan Province (117-02001001002107), College Student Innovation and Entrepreneurship Training Project of Yunnan (2017), College Student Innovation and Entrepreneurship Training Project of China (201710691001), Youth Fund Project of Yunnan Minzu University (2017QN09) Graduate Student Innovation and Entrepreneurship Training Project of Yunnan Minzu University (2018).

#### References

- [1] Z.D. Zhang, The status and prospect of bamboo resources in China, *Land Vires.*, 4 (1998) 12–13.
- [2] M. Ahmaruzzaman, S.L. Gayatri, Batch adsorption of 4-nitrophenol by acid activated jute stick char: equilibrium, kinetic and thermodynamic studies, *Chem. Eng. J.*, 158 (2010) 173–180.
- [3] O. Gimeno, M. Carbajo, F.J. Beltrán, F.J. Rivas, Phenol and substituted phenols aops remediation, *J. Hazard. Mater.*, 119 (2005) 99–108.
- [4] J. Luan, A. Plaisier, Study on treatment of wastewater containing nitro phenol compounds by liquid membrane process, *J. Membr. Sci.*, 229 (2004) 235–239.
- [5] P. Bergauer, P.A. Fonteyne, N. Noland, F. Schinner, R. Margesin, Biodegradation of phenol and phenol-related compounds by psychrophilic and cold-tolerant alpine yeasts, *Chemo.*, 59 (2005) 909–918.
- [6] M. Afzal, S. Iqbal, S. Rauf, Z.M. Khalid, Optimization of an open-focused microwave oven digestion procedure for determination of metals in diesel oil by inductively coupled plasma optical emission spectrometry, *J. Hazard. Mater.*, 149 (2007) 60.
- [7] Q. Miao, Y. Tang, J. Xu, X. Liu, L. Xiao, Q. Chen, Activated carbon prepared from soybean straw for phenol adsorption, *J. Taiwan Inst. Chem. Eng.*, 44 (2013) 458–465.
- [8] T.R. Bastami, M.H. Entezari, Activated carbon from carrot dross combined with magnetite nano particles for the efficient removal of p-nitrophenol from aqueous solution, *Chem. Eng. J.*, 210 (2012) 510–519.
- [9] M.A.W.D. Wan, A.H. Houshamnd, Textural characteristics, surface chemistry and oxidation of activated carbon, *Energy Chem.*, 19 (2010) 267–279.
- [10] L.M. Cotoruelo, M.D. Marqués, F.J. Díaz, J. Rodríguez-Mirasol, J.J. Rodríguez, T. Cordero, Adsorbent ability of lignin-based activated carbons for the removal of p-nitrophenol from aqueous solutions, *Chem. Eng. J.*, 184 (2012) 176–183.
- [11] Test methods of wooden activated carbon determination of iodine number. GB/T 12496.8-1999.
- [12] Test methods of wooden activated carbon determination of methylene blue adsorption. GB/T 12496.10-1999.
- [13] B. Cagnon, X. Py, A. Guillot, The effect of the carbonization/activation procedure on the micro porous texture of the subsequent chars and active carbons, *Micropor. Mesopor. Mater.*, 57 (2008) 273–282.
- [14] Y.J. Zhang, Z.J. Xing, Z.K. Duan, Effects of steam activation on the pore structure and surface chemistry of activated carbon derived from bamboo waste, *Appl. Sur. Sci.*, 315 (2014) 279–286.
- [15] A.C. Lua, J. Guo, Preparation and characterization of activated carbons from oil-palm stones for gas-phase adsorption, *Colloids Surf. A Physicochem. Eng. Asp.*, 179 (2001) 151–162.
- [16] C. Bouchelta, M.S. Medjram, M. Zoubida, Effects of pyrolysis conditions on the porous structure development of date pits activated carbon, *J. Anal. Appl. Pyro.*, 94 (2012) 215–222.
- [17] H.P. Zhang, Y.E. Li, L.C. Yang, Preparation of activated carbon from coconut shell by physical activation, *J. Xiamen Univ.*, 43 (2004) 833–835.
- [18] G. Li, J. Li, W. Tan, H. Jin, H. Yang, J. Peng, Preparation and characterization of the hydrogen storage activated carbon from coffee shell by microwave irradiation and KOH activation, *Inter. Bioterior Biodegrad.*, 113 (2016) 386–390.
- [19] Y.B. Tang, Q. Liu, F.Y. Chen, Preparation and characterization of activated carbon from waste ramulus mori, *Chem. Eng. J.*, 203 (2012) 19–24.
- [20] K. Sathish-Kumar, G. Vázquez-Huerta, A. Rodríguez-Castellanos, H.M. Poggi-Varaldo, O. Solorza-Feria, Microwave assisted synthesis and characterizations of decorated activated carbon, *Inter. J. Electrochem. Sci.*, 7 (2012) 5484–5494.
- [21] Q.S. Liu, Z. Tong, W. Peng, G. Liang, Preparation and characterization of activated carbon from bamboo by microwave-induced phosphoric acid activation, *Indust. Crops Prod.*, 31 (2010) 233–238.
- [22] K. Murashko, D. Nevstrueva, A. Pihlajamäki, T. Koiranen, J. Pyrhönen, Cellulose and activated carbon based flexible electrical double-layer capacitor electrode: preparation and characterization, *Energy*, 119 (2017) 435–441.
- [23] K.G. Rekha, R. Radhika, T. Jayalatha, S. Jacob, R. Rajeev, B.K.-George, Removal of perchlorate from drinking water using granular activated carbon modified by acidic functional group: adsorption kinetics and equilibrium studies, *Pro. Safe. Environ. Protec.*, 109 (2017) 158–171.
- [24] X.Y. Fang, G.Z. Li, J.X. Li, H. Jin, J. Veeriah, S. Li, H.B. Wang, M. Yang, Bamboo charcoal derived high-performance activated carbon via microwave irradiation and KOH activation: application as hydrogen storage and super-capacitor, *Desal. Water Treat.*, 96 (2017) 120–127.
- [25] H.M. Xie, T.T. Gao, X. Tang, Y. Deng, S.U. Hong-Fang, Y.L. Shen, On adsorption performances of iron modified activated carbon for p-nitrophenol in waste water, *J. Southwest China Normal Univ.*, 37 (2012) 118–122.
- [26] S. Mor, K. Chhoden, P. Negi, K. Ravindra, Utilization of nano-alumina and activated charcoal for phosphate removal from wastewater, *Environ. Nanotech. Mon. Manage.*, 7 (2017) 15–23.
- [27] W.J. Zheng, J.W. Lin, Y.H. Zhan, H. Wang, Adsorption characteristics of nitrate and phosphate from aqueous solution on zirconium-hexadecyltrimethylammonium chloride modified activated carbon, *Environ. Sci.*, 36 (2015) 2185–2194.

- [28] B. Liu, J. Gu, Y.Y. Tu, J.B. Zhou, Adsorption property of activated carbon from leaves of phoenix tree on different polarity phenols, *Res. Environ. Sci.*, 27 (2014) 92–98.
- [29] S. Langergren, B.K. Svenska, Zur theorie der sogenannten adsorption gelöster stoffe, *Veter. Handlin.*, 24 (1898) 1–39.
- [30] Y.S. Ho, G. McKay, Pseudo-second order model for sorption processes, *Process Biochem.*, 34 (1999) 451–465.
- [31] Y.S. Ho, Review of second-order models for adsorption systems, *Chem.*, 136 (2006) 681–689.
- [32] I. Langmuir, The adsorption of gases on plane surfaces of glass, mica and platinum, *J. Chem. Phys.*, 40 (2015) 1361–1403.
- [33] H.M.F. Freundlich, Über die adsorption in lösungen, *Z. Phys. Chem.*, 57 (1906) 384–470.
- [34] X. Ge, F. Tian, Z. Wu, Adsorption of naphthalene from aqueous solution on coal-based activated carbon modified by microwave induction: Microwave power effects, *Chem. Eng. Pro.*, 91 (2015) 67–77.
- [35] X. Ge, Z. Wu, Microwave-assisted modification of activated carbon with ammonia for efficient pyrene adsorption, *J. Indus. Eng. Chem.*, 39 (2016) 27–36.
- [36] M.J. Ahmed, S.K. Theydan, Microwave assisted preparation of micro porous activated carbon from Siris, seed pods for adsorption of metronidazole antibiotic, *Chem. Eng. J.*, 214 (2013) 310–318.
- [37] K.Y. Foo, B.H. Hameed, Microwave-assisted regeneration of activated carbon, *Bio. Technol.*, 119 (2012) 234.